A Novel Approach to Modeling of Interfacial Fiber/Matrix Cyclic Debonding

Paria Naghipour[1], Evan J. Pineda[2], Steven M. Arnold[2]

Abstract: The micromechanics theory, generalized method of cells (GMC), was employed to simulate the debonding of fiber/matrix interfaces, within a repeating unit cell subjected to global, cyclic loading, utilizing a cyclic crack growth law. Cycle dependent, interfacial debonding was implemented as a new module to the available GMC formulation. The degradation of interfacial stresses with applied load cycles was achieved via progressive evolution of the interfacial compliance A periodic repeating unit cell, representing the fiber/matrix architecture of a composite, was subjected to combined normal and shear loadings, and degradation of the global transverse stress in successive cycles was monitored. The obtained results were compared to values from a corresponding finite element model. Reasonable agreement was achieved for combined normal and shear loading conditions, with minimal variation for pure loading cases. The higher variation in mixed loading cases was attributed to the uncoupled normal/shear formulation of GMC, and can be further improved by using available high fidelity options.

1   Introduction

Failure analysis using micromechanics model representing repeating unit cells (RUCs) or representative volume elements (RVEs) is considered as a promising tool to study the mechanical behavior of complex, heterogeneous materials. The deformation and failure of a unit cell representing the microstructure, provides the opportunity to capture local phenomena more accurately under a globally applied loading. Furthermore, the microscale analyses can be linked to larger scales to provide robust, multiscale prediction tools. Numerous studies in literature have used micromechanics as a tool to predict homogenized material properties, or model localized failure behavior.

Following very early studies by Eshelby [Eshelby (1957)] to predict the larger scale macro-mechanical effective properties of composites using microscale analytical

---

[1] Ohio Aerospace Institute, 22800 Cedar Point Road, Brook Park, OH 4414.
[2] NASA Glenn Research Center, 21000 Brookpark Road, Cleveland, OH 44135.

models, Christensen and Lo [Christensen and Lo (1979)] developed an analytical model, consisting of a micro-mechanical 3-dimensional spherical/2-dimensional cylindrical composite sphere/cylinder model, to predict effective shear properties of a three-phase composite successfully. Similarly, Dvorak [Dvorak (1992)] proposed a novel method, derived from the representation of local stress and strain fields by novel transformation influence functions and concentration factor tensors, to evaluate local fields and overall inelastic properties of a composite. Later, Michel and Suquet [Michel and Suquet (2003)] expanded the aforementioned uniform transformation field analysis of Dvorak [Dvorak (1992)] to non-uniform transformation fields. The accuracy of the proposed model in predicting effective mechanical behavior of composites was verified via comparison to numerical simulations. Similarly, McCartney and Kelly [McCartney and Kelly (2007)] applied sets of explicit, analytical formulae (based on the concentric cylinder model of fiber and matrix [Hashin (1983)]) to predict the effective elastic and thermal properties for angle-ply composite laminates with various ply angles.

Furthermore, in the context of semi-analytical micromechanics, Bednarcyk, Aboudi, and Arnold (2010) implemented a multiaxial continuum damage model into the high-fidelity generalized method of cells (HFGMC) [Aboudi J, Pindera M-J, Arnold S.M. (2001)] micromechanics theory to predict the response of a glass/epoxy composite under combined loading. Pineda, E.J., Bednarcyk, Waas, and Arnold (2013) incorporated a crack band model by Bazant and Oh (1983) into the generalized method of cells (GMC) [Paley and Aboudi (1992)] and HFGMC to capture local failure in a manner that is insensitive to refinements in the discretization of the RUC, and verified the response of an RUC under combined loading against an analogous, fully numerical, finite element method (FEM) model. Expanding upon previous works of Aboudi (1987), Sankurathri, A., Baxter S, Pindera M-J (1996) and Achenbach, and Zhu (1989), Bednarcyk and Arnold (2000) developed an evolving compliant interface (ECI) model within GMC to predict fiber/matrix debonding in metal matrix composites. Kurnatowski and Matzenmiller (2012) utilized traction separation laws to govern the behavior of the fiber/matrix interface within a GMC RUC.

In addition to analytical and semi-analytical methods, several authors have studied micro-mechanics of damage and failure of composites, utilizing FEM. Sun and Vaidya (1996) introduced a mechanics approach using an RVE to predict the mechanical properties of unidirectional fiber composites, wherein the local, non-homogeneous stress and strain fields of the RVE were related to the average stresses and strains using Gauss theorem and strain energy equivalence principle (within the FE context). Belytschko, Loehnert, and Song (2008) used perforated unit cells (excluding subdomains that are unstable in atomistic or discrete finer scales) within an

extended finite element (XFEM) framework to compute an equivalent discontinuity/jump at the coarser scale, including both the direction and magnitude of the discontinuity. Their method has been successfully employed to simulate the growth of fatigue cracks in a unit cell and the corresponding coarse-grain discontinuities. Alfaro, Suiker, and De Borst (2010) studied the transverse failure response of a single-fiber unidirectional fiber-epoxy RUC by means of interface damage models placed at the fiber/matrix boundary. The simulated fracture patterns, shown to be in good agreement with experimental observations, demonstrated the influence of the local, fiber/matrix interfacial strength on the global, transverse failure response. Gonzalez and Llorca (2006) simulated the fracture behavior of a fiber-reinforced notched composite beam by means of an embedded-cell musltiscale approach, where the region surrounding the notch tip (stress concentration point) was composed of the actual fiber/matrix topology in the composite, while the rest of the beam was represented by a homogeneous transversely isotropic solid. The simulation results were in good agreement with the experimental data at both the microscopic and the macroscopic level, showing the predictive capability of this approach in simulating quasi-static fracture mechanisms Later Mishnaevsky and Brondsted (2007) used an automated generation of 3D FEM micromechanical models of composites with predefined parameters for the microstructure (fiber/matrix) and analyzed the fiber fracture and interfacial damage evolution (with pre-introduced matrix cracks) based on maximum principal stress predefined fracture planes. Using a similar approach as Gonzalez and Llorca (2006), Totry, Molina, González, and Llorca (2010) studied the effect of constituent properties (fibers, matrix and interface), on the in-plane shear behavior and strength of carbon-fiber reinforced composites through a combination of experiments and numerical simulation. Fiber and matrix spatial distribution within the lamina were taken in to account explicitly through the representative microstructure. In addition, the actual failure mechanisms (plastic deformation of the matrix and interface decohesion) were included in the simulations. Very good agreement was observed between experiments and numerical simulation. Later Totry, González, and Llorca (2008) successfully analyzed the failure locus of a composite lamina subjected to transverse compression and out-of-plane shear, and the further influence of the loading path on the failure locus, using a similar representative microstructure methodology. Gamstedt and Sjorgen (1999) designated the adverse effect of compressive load excursions under low cycle fatigue for a single fiber glass-epoxy specimen by counting transverse cracks experimentally, and verifying their results through FEM. However, the FEM model did not take the crack tip energy release rates and the ongoing fracture/damage mechanisms in to account. The crack opening zone, compared to the experimental results, was based on a stress-based failure analysis.

The mentioned works have presented successful predictions of effective composite properties or quasi-static failure behavior of composites using micromechanics-based approaches. Nevertheless, none of them has directly addressed numerical modeling of fiber/matrix debonding due to fatigue in detail, taking the micromechanics of the ongoing interfacial damage in to account (a significant damage evolution scenario in composites). Moreover, the methods utilizing FEM are computationally expensive, especially if a large number of elements is required for a numerically converged FEM analysis of the unit cell.

The main novelty of this work was employing the micromechanics model (GMC) to simulate of the cyclic cracking of the fiber/matrix interface utilizing a Paris-type [Paris and Erdogan (1963)], cyclic crack/debonding growth law. Within GMC, the microstructure of a periodic material is represented by a rectangular repeating unit cell consisting of an arbitrary number of rectangular subcells, each of which may be a distinct material obeying any constitutive law. As presented in detail in previous literature [Aboudi (1987); Bednarcyk and Arnold (2000)], this method is semi-analytical in nature and its formulation involves application of several continuity conditions in an average sense. Because of this averaging, and due to a decoupling of normal and shear field components, the model can be less accurate than traditional finite element analysis (FEA), if shear-normal coupling is significant, but it is incredibly computationally efficient, offering solution times that are appreciably faster . Moreover, GMC provides a distribution of the local fields in composite materials (an advantage over traditional, mean field, micromechanics theories) allowing incorporation of arbitrary inelastic constitutive models for the composite phases, as well as other microscale effects such as fatigue damage and debonding. Furthermore, the GMC solution is completely insensitive to refinements in the subcell mesh if the geometry is fixed. During cyclic debonding, a distinction needs to be made between the loading and unloading paths allowing for hysteresis. Within the context of GMC, this physical phenomenon is represented mathematically by governing the evolution of the interfacial compliance with the number of global load cycles (with the help of Paris-type cyclic crack/debonding growth law). The Paris-type fatigue fracture law has been successfully implemented and experimentally validated by Naghipour, Bartsch, and Voggenreiter (2011) within the context of FE cohesive zone formulation to simulate the interfacial damage of composites, and is used as a numerical validation tool for this study.

In Section 2, the constitutive response of an interface exhibiting cyclic damage is described concisely. In section 3, the constitutive response is used to formulate the cyclic, damage evolution law for the interfacial compliance utilized implemented in GMC. Construction of the RUC models, applied boundary conditions and results obtained through GMC are compared to FEM and presented in Section 4. Finally

a brief summary and conclusion is given in Section 5.

2 Constitutive response

Modeling cyclic debonding of fiber/matrix interface is accomplished through a cyclic cohesive zone formulation developed by Naghipour, Bartsch, and Voggenreiter (2011) for capturing mixed mode interfacial fatigue damage of CFRPs. Cohesive zone theory, for prediction of crack initiation and propagation, was first suggested by Dugdale (1960), and later Barenblatt (1962) and Hillerborg, Modeer, Petersson (1976) added significant contributions. Since then, many authors have been working actively on improving the approach or, within an FEM setting, development of interface elements [Foulk, Allen, and Helms (2000); Ladeveze, Guitard, Champaney, and Aubard (2000); Allix and Blanchard (2006); Borg, Nilsson, and Simonsson (2002); Alfano and Crisfield (2001); Turon, Camanho, Costa, and Davila (2006)]. When subjected to cyclic loading, the constitutive law of the interface element (relating interfacial tractions τ, to interfacial displacement, δ) must be reformulated to account for subcritical damage accumulation and stiffness degradation within subsequent unloading–reloading steps (Fig. 1)
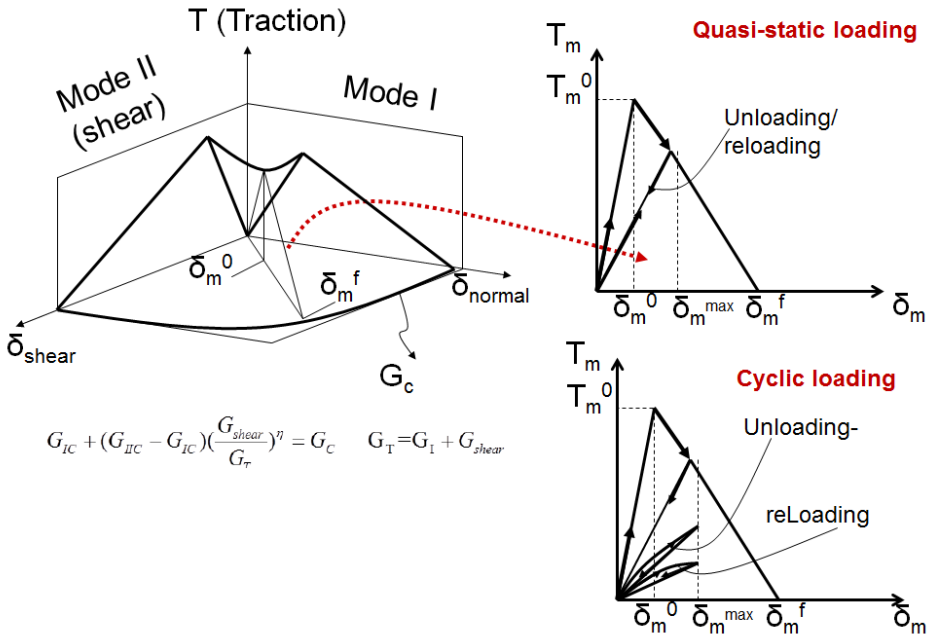
Figure 1: Cohesive law for mixed mode delamination with linear softening

τ_m and δ_m are mixed mode interfacial tractions and displacement respectively. τ_m is the corresponding interfacial strength and δ_m corresponds to damage initiation (mixed mode opening displacement or the fictive crack tip). The initiated damage then starts evolving based on an energy based propagation criterion, utilizing normal and shear fracture energies (G_I and G_{shear}) until the final failure point is reached (Fig. 1). Normal and shear mode fracture energies shall be measured through mixed mode fracture experiments for the required mode mixity. The detailed formulation of the interfacial constitutive behavior is given in [Naghipour, Bartsch, and Voggenreiter (2011)], and incorporated into an FEM element, and will only be shortly reviewed here. The model is based on a cohesive law that links fracture and damage mechanics to establish the evolution of the damage variable in terms of the crack growth rate *da/dN*. The model relates damage accumulation to the number of load cycles while taking into account the loading conditions. According to Naghipour et al. [Naghipour, Bartsch, and Voggenreiter (2011)] by implementing a cyclic damage variable in the cohesive interface response, the cyclic crack growth and stiffness/stress degradation can be captured properly. In order to define the evolution of the damage variable within successive cycles ($\partial d/\partial N$), the crack/ cracked area growth rate under fatigue loading, $\partial A/\partial N$, which is a load and material-dependent characteristic in the Paris law is embedded in the formulation of the interfacial behavior as shown in Equation. (1).

$$\frac{\partial A}{\partial N} = C\left(\frac{\Delta G}{G_c}\right)^m \tag{1a}$$

$$\frac{\partial d}{\partial N} = \left\{ \begin{array}{l} \frac{1}{A_{cz}} \frac{(\delta_m^f(1-d)+d\delta_m^0)^2}{\delta_m^f \delta_m^0} C\left(\frac{\Delta G}{G_c}\right)^m \quad G_{th} < G_{max} < G_c \\ 0 \end{array} \right\} \tag{1b}$$

d stands for the damage variable, δ_m^0 for initial displacement at delamination onset, and final separation displacement is designated by δ_m^f (Fig. 1). C, m, and G_{th} are Paris plot parameters that are obtained by plotting $\partial A/\partial N$ versus cyclic variation in the energy release rate, ΔG, on log-log scale. G_c is the total mixed mode fracture toughness, determined from fracture toughness experiments. A_{CZ} stands for the cohesive zone area, a constant averaging factor which might be calibrated back from available experimental fracture data The maximum cyclic variation in the energy release rate ΔG can be computed by the constitutive law of the cohesive zone model as given in detail by Naghipour et. al [Naghipour, Bartsch, and Voggenreiter (2011)]. Taking this in to the formulation of the cyclic evolution of the damage

parameter, final form of Equation (1) can be rewritten as:

$$\frac{\partial d}{\partial N} = \left\{ \begin{array}{l} \frac{1}{A_{cz}} \frac{(\delta_m^f(1-d)+d\delta_m^0)^2}{\delta_m^f \delta_m^0} C \left(\frac{\frac{\tau_m^0}{2}\left(\delta_m^0 + \frac{(\delta_m^f - \delta_m^{\max})^2}{\delta_m^f - \delta_m^0}\right)(1-R^2)}{G_c} \right)^m \quad G_{th} < G_{\max} < G_c \\ \\ 0 \end{array} \right\}$$

(2)

This interfacial fatigue damage model was implemented as a User element (UEL) in the FE code Abaqus, and provides promising results for cyclic degradation of the interfacial stress [Naghipour, Bartsch, and Voggenreiter (2011)].

3   Development of cyclic compliant interface model

The micromechanics model employed to simulate the fatigue debonding of fiber/matrix interfaces is the GMC, developed by Paley and Aboudi (1992). The geometry of a doubly-periodic GMC RUC is shown in Fig. 2, wherein the microstructure of a periodic material is represented by a rectangular repeating unit cell consisting of an arbitrary number of rectangular subcells, each of which may be a distinct material. The methodology of GMC is described thoroughly by Paley and Aboudi (1992) and Arnold and Bednarcyk (2002).

The debonding methodology of GMC employs the concept of a flexible interface wherein a discontinuity in the normal or tangential displacement component at an interface, I, is permitted. These discontinuities are taken to be proportional to the appropriate stress component at the interface such that,

$$[u_n]^I = R_n \sigma_n|^I \quad \sigma_n = \sigma_{DB}^n \tag{3}$$

$$[u_t]^I = R_t \sigma_t|^I \sigma_t = \sigma_{DB}^t \tag{4}$$

In Equations (3-4), $[u_n]^I$ and $[u_t]^I$ are the normal and tangential displacement discontinuities at the interface, with $\sigma_n|^I$ and $\sigma_t|^I$ as corresponding interfacial stresses, R_n and R_t are debonding parameters representing the effective compliance of the interface, and σ_{DB}^n and σ_{DB}^t are the normal and tangential strengths of the interface. The flexible interface model was originally implemented into the method of cells by Aboudi (1987) and GMC by Sankurathri, A., Baxter S, Pindera M-J (1996). Debonding was restricted if the interface was subjected to compression by Achenbach and Zhu (1989). The flexible interface model was further extended by Bednarcyk and Arnold (2000, 2002)], Bednarcyk, Arnold, Aboudi, and Pindera
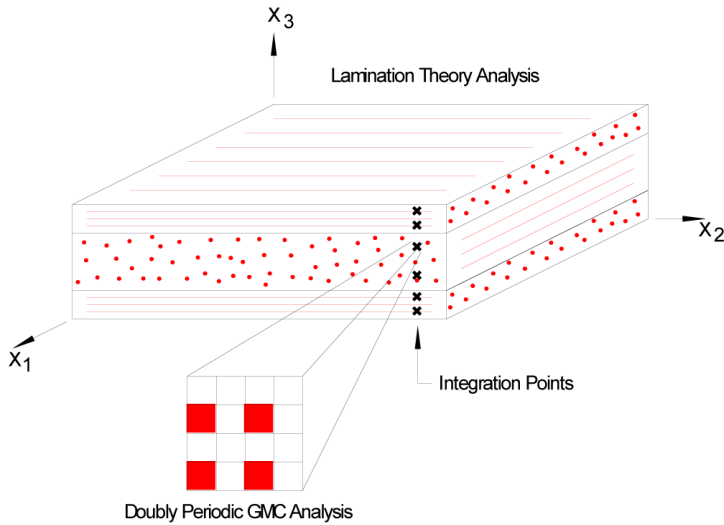
Figure 2: Schematic showing the lamination theory geometry with GMC embedded to represent the behavior of the composite material at the through-thickness integration points

(2004) to the evolving compliant interface (ECI) model by incorporating time dependent interfacial compliances ($R_n(t)$ and $R_t(t)$). Pineda (2012) formulated an interfacial compliance evolution law that was implicitly dependent on the traction versus separation response of the interface. Kurnatowski and Matzenmiller (2012) implemented a similar interfacial compliance model within GMC and used it to predict fiber/matrix debonding in a composite using interfacial fracture toughness parameters as inputs.

Here, a new interfacial compliance will be formulated using the previously described fatigue damage model. Similar to the fatigue cohesive FE model developed in Naghipour, Bartsch, and Voggenreiter (2011), the cyclically evolving interfacial compliance is defined through the linking of damage and fracture mechanics. Embedding a cyclic fracture law, such as Paris law [Paris and Erdogan (1963)], in to the interfacial compliance formulation enables us to set up a physics-based, cyclic debonding model. As a start point, the cyclic evolution equation can be written as:

$$\frac{\partial R}{\partial N} = \frac{\partial R}{\partial A} \frac{\partial A}{\partial N} \tag{5}$$

A represents the debonding area, and *dA/dN* is the growth rate of the damaged

(debonded) area. Using chain rule, Equation (4) can be rewritten as:

$$\frac{\partial R}{\partial N} = \frac{\partial R}{\partial \sigma}\frac{\partial \sigma}{\partial A}\frac{\partial A}{\partial N} \tag{6}$$

The first part of Equation (5) (rate of change of compliance with the debonded area, *dR/dA*) can be calculated analytically if a linear descent is assumed for the debonding stress versus displacement (see Fig. 3 below):
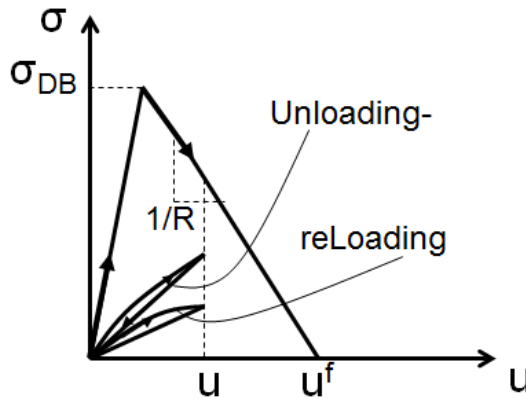
Figure 3: Linear descent of the interfacial debonding (interfacial stress versus displacement)

A is the debonded area under Fig. 3 from the debond initiation up to a specified displacement (*u*). It should be noted that since the interfacial debonding is based upon the interfacial compliance, no initial, fictitious stiffness required for the interface (as is needed for FEM cohesive elements), and the adjacent subcells are perfectly bonded, automatically. The derivative of the compliance with respect to debonding stress (*dR/dσ*) reads:

$$\frac{\partial R}{\partial \sigma} = \frac{-u_c}{\sigma^2} \tag{7}$$

Considering Fig. 3, the debonded area can be defined in terms of debonding stress:

$$A = \frac{\sigma + \sigma_c}{2}(\sigma - \sigma_c)\frac{-u_c}{\sigma_c} \tag{8}$$

Using Equation (7), the derivative of the debonding stress with respect to the debonding area is

$$\frac{\partial \sigma}{\partial A} = -\frac{\sigma_c}{\sigma u_c} \tag{9}$$

Substituting Equation (8) and (6) into the definition of *dR/dA* (Equation (4)), we obtain:

$$\frac{\partial R}{\partial A} = \frac{\sigma_c}{\sigma^3} \tag{10}$$

In analogy to the second part of Equation (4), *dA/dN*, represents a Paris-type equation relating the fatigue growth of the debonding area to strain energy release rate. Under cyclic loading, the debonded area grows as the number of cycles increases. It can be assumed that the increase in cracked area is equivalent to the increase in the debonded area of all of the involved interfaces. Therefore, the crack growth rate in Paris-type law can be assumed equal to sum of the debonded area growth rates of all debonded subcells. Assuming a mean value for the debonded area growth rate ($\tilde{A}_d$) and assuming the mean area of the subcell interfaces does not change significantly (can be assumed as constant) the second part of Equation (4) can be rewritten as:

$$\frac{\partial A}{\partial N} = \sum \frac{\partial A_{debonded}}{\partial N} = m \frac{\partial \tilde{A}_d}{\partial N} \tag{11}$$

m is an averaging coefficient analogous to *Acz* in Equation (2), which can be calibrated back from available experimental results. For simplicity, both *m* and *Acz* are assumed to be 1 here. ($d\tilde{A}_d/dN$) is approximated using the Paris-type law, and dA/dN can then be rewritten as:

$$\frac{\partial A}{\partial N} = mC^{Paris} \left(\frac{\Delta G}{G_c} \right)^{m^{Paris}} \tag{12}$$

C^{Paris}, m^{Paris}, and G_c are material parameters that depend on the failure mode (normal, shear or combination of both), and *G* is the strain energy release rate (dG=σdu). Substituting u=Rσ from Equation (3), and using the chain rule derivative, Equation (12) can be rewritten as:

$$\frac{\partial A}{\partial N} = mC^{Paris} \left(\frac{dR\sigma + Rd\sigma}{G_c} \right)^{m^{Paris}} \tag{13}$$

The compliance increment (*dR*), current compliance (*R*), stress (σ) and stress increment (*dσ*) are updated throughout GMC. However, an initial non-zero value must be assumed for the initial compliance increment. Accordingly, a threshold value (G_{th}) is introduced, and debonding is precluded if the strain energy release rate is smaller than the fatigue threshold of the strain energy release rate. In the GMC context, this threshold value will be approximated from the micro-level matrix-matrix damage sub-model.

4 Results and Discussion

In order to numerically validate the predictive capability of the newly implemented cyclic debonding module in GMC, a one to one comparison to analogous finite element simulations was carried out. The successive degradation in the global transverse stress, caused by interfacial fatigue debonding of the fiber/matrix, was compared for corresponding GMC and FEM simulations. Pure normal, pure shear and various mixed mode (normal plus shear) loadings were applied to verify the accuracy of the model, under combined effects of normal and shear loads (0% mode mixity corresponding to pure normal loading and 100% to pure shear). The GMC model consisted of a doubly-periodic, square-packed RUC subjected to strain driven, cyclic loading (Fig. 4a).
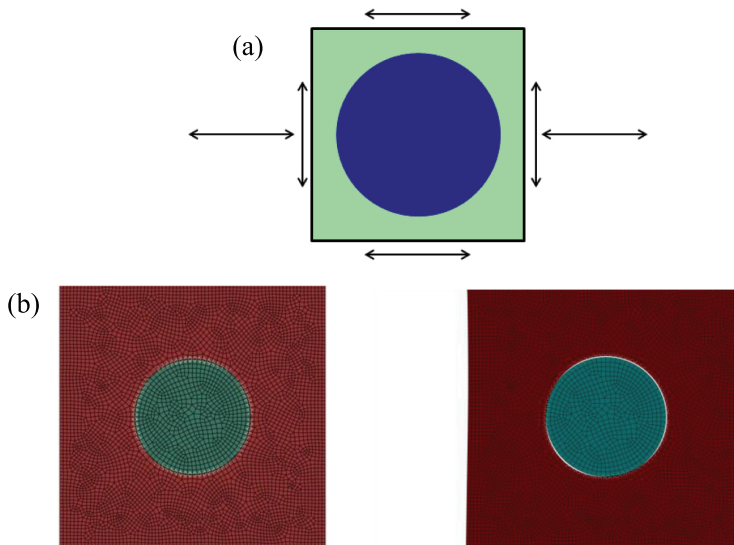
Figure 4: (a) A schematic representation of a fiber/matrix RUC subjected to combined normal and shear loading; (b) A schematic representation of an undefomed and deformed fiber/matrix RUC (separated interface).

The RUC was composed of 14 subcells x 14 subcells. A convergence study was conducted, and this architecture represented the least refined RUC that provided a converged solution. The fiber volume fraction of the RUC was 60% for both the FEM and GMC models. Since the debonding formulation uses energy release rates, it is important to use realistic dimensions for the RUC. Therefore a typical fiber radius of 5μm was chosen for both the FEM and GMC models. Similarly, the

FEM model of the RUC, a 2-D model composed of 2-D generalized plane strain elements with an elastic anisotropic fiber and isotropic matrix with user-defined cohesive elements [Naghipour, Bartsch, and Voggenreiter (2011)] placed at the fiber/matrix interface, was subjected to the same loading conditions. Exemplary undeformed and deformed FE meshes are shown in Fig.4b. The fiber/matrix interface separation continues growing until interfacial tractions reach a plateau state. The degradation of the global transverse stress was monitored as number of cycles grew. The total amplitude of the displacement/strain-controlled cyclic loading was assumed to be 5e-4 mm. Convergence in the FEM simulation was achieved using a 75 element x 75 element mesh, which is computationally very costly, but necessary for achieving accurate results. The repeating nature of the fiber/matrix geometry is taken in to consideration via applying periodic boundary conditions in the FE and GMC simulations (periodic boundary conditions are automatically assumed in the GMC formulation). It is worth mentioning that the same parameters for the matrix (epoxy 8552), fiber (carbon), and interface, obtained partially from available sources in literature were used in GMC and the FEM simulation. Unfortunately very few experimental studies are have addressed cyclic micro-level fiber/matrix measurements [(Gamstedt and Sjorgen (1999)], and meanwhile the values are not reported explicitly. Therefore, the interface parameters are assumed to be close to the available measurements in macro level obtained from authors's previous experimental results [Naghipour, Bartsch, and Voggenreiter (2011)].

Table 1: Properties used in GMC and FEM simulations

Mechanical properties of epoxy 8552				
E_{11} (MPa)	ν_{12}	G_{12} (MPa)		
3450	0.35	1270		
Mechanical properties of fiber (Carbon AS4)				
E_{11}(GPa)	E_{22}(GPa)	ν_{12}	G_{12} (GPa)	G_{23} (GPa)
388.2	7.6	0.4	15	9
Properties of interface (UEL and GMC) C^{Paris} =0.0616 mm/cycle m^{Paris} =1.15 G_{th}= 0.001 mJ/ mm^2 Total G_c = 0.8 mJ/mm^2 ΔN=1 m=1				

The user-developed cohesive element in FEM has been demonstrated the reliable and predictive capability to capture the cyclic delamination growth according to Naghipour et al. [Naghipour, Bartsch, and Voggenreiter (2011)], and therefore was used as a validation tool. A comparison of the GMC and FEM results is presented in Fig. 5. Very good agreement of stress degradation in subsequent cycles was achieved, when comparing the fiber/matrix debonding in GMC with the corresponding FEM simulations (Fig. 5) for various normal/ shear combinations. The

variation in results was higher for combined normal and shear loading cases, with a mean relative error value of 12%, compared to pure normal or pure shear loadings (mean relative error value of 5%). The interfacial debonding formulation incorporated a coupled, mixed-mode fracture energy evolution law. However, in GMC the normal and shear stresses are uncoupled; i.e., when a purely normal stress state is applied, only normal stresses will develop locally, and vice versa. Thus, under combined applied normal-shear loading cases, the error introduced by the lack of local normal-shear stress coupling is exacerbated when a mixed-mode fracture energy evolution law is utilized because the stresses that should arise due to coupling, and would contribute significantly to the overall degradation of the interface, are absent. Under pure normal or shear loading, the degradation due to the stresses arising from coupling is a second order effect.

However, the relatively low computational cost of the cyclic debonding analysis in GMC compensates for the mentioned modest error values. For the pure normal case the FEM runtime was 16425 seconds, whereas, the GMC solution was obtained in 180 seconds. On average, the GMC solution was about 90 times faster than the FE solution. If fidelity is valued over efficiency, HFGMC can be employed at an added computational expense. The stress degradation calculated through GMC is higher compared to FE results for all loading cases, which shows the consistency of both solutions.
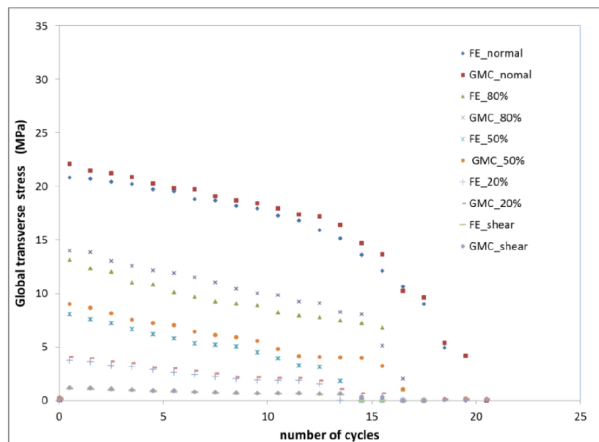
Figure 5: Degradation of the global transverse stress versus number of cycles for different combinations of normal and shear modes (various mode mixities) comparison between FE and GMC results

5   Conclusion

Simulation of debonding of the fiber/matrix interface due to cyclic loading, via implementation a fatigue crack growth law in to the available formulation of GMC, was accomplished, and the results were compared to a previously, experimentally validated fatigue delamination FE model. The stress degradation in subsequent cycles is captured with minimal error for pure cyclic normal/ shear loading cases when comparing the fiber/matrix debonding in GMC with the corresponding FE simulations. The higher variation in results for combined normal/ shear loading cases is probably due to the uncoupled normal and shear stresses formulation in GMC. However, the exceptionally higher computational efficiency achieved by using GMC compensates for the mentioned error values.

References

Aboudi, J. (1987): Damage in composite modeling of imperfect bonding. *Compos. Sci. Technol.* Vol. 28, pp. 103-128.

Aboudi, J; Pindera, M-J; Arnold, S.M. (2001): Linear thermoelastic higher-order theory for periodic multiphase materials. *J. Appl. Mech,* Vol. 68, pp. 697-707.

Achenbach, J. D.; Zhu, H. (1989): Effect of interfacial zone on mechanical behavior of failure of fiber-reinforced composites. *J. Mech. Phys. Solids.* Vol. 37, pp. 381-393.

Alfaro, M.V.C.; Suiker, A.S.J.; De Borst R. (2010): Transverse failure behavior of fiber-epoxy systems. *Journal of Composite Materials.* Vol. 44, pp. 1493-1516.

Alfano, G.; Crisfield, MA. (2001): Finite element interface models for delamination analysis of laminated composites: mechanical and computational issues. *Int J Num Meth Eng.* Vol. 50, pp. 1701–1736.

Allix, O.; Blanchard L. (2006): Mesomodeling of delamination: towards industrial applications. *Compos Sci and Tech.* Vol. 66, pp. 731-744.

Barenblatt, GI. (1962): The mathematical theory of equilibrium cracks in brittle fracture. Adv Appl Mech Vol. 7. pp. 55–129.

Bazant, Z.P.; Oh, B.H. (1983) Crack band theory for fracture of concrete. *Matriaux et Constructions* Vol. 16 - 93.

Bednarcyk, B.A.; Aboudi, J.; Arnold, S.M. (2010): Micromechanics Modeling of Composites Subjected to Multiaxial Progressive Damage in the Constituents. *AIAA JOURNAL* Vol. 48, No. 7, pp. 1367-1378.

Bednarcyk, B.A.; Arnold, S.M. (2000): A New Local Debonding Model With

Application to the Transverse Tensile and Creep Behavior of Continuously Reinforced Titanium Composites. *NASA/TM*—2000-210029.

Bednarcyk, B.A.; Arnold, S.M. (2002): MAC/GMC User Guide: Version 4.0. *NASA/TM*-2002-212077.

Bednarcyk, B.A.; Arnold, S.M. (2002): Fully coupled micro/macro deformation, damage, and failure prediction for sic/ti-15-3 laminates. *Journal of aerospace Engineering,* Vol. 15, pp. 74-83.

Bednarcyk, B.A.; Arnold, S.M.; Aboudi, J.; Pindera, M-J. (2004): Local field effects in titanium matrix composites subject to fiber-matrix debonding. *International Journal of Plasticity*, Vol. 20, pp. 1707–1737.

Belytschko, T.; Loehnert, S.; Song, J-H. (2008): Multiscale aggregating discontinuities: A method for circumventing loss of material stability. *Int. J. Numer. Meth. Engng* Vol. 73, pp. 869–894.

Borg, R.; Nilsson, L.; Simonsson K. (2002): Modeling of delamination using a discretized cohesive zone and damage formulation. *Compos Sci and Tech,* Vol. 62, pp. 1299–1314.

Christensen, R.M.; Lo, K.H. (1979) Solutions for effective shear properties in three phase sphere and cylinder models. *J. Mech. Phys. Solids*. Vol. 27, pp. 315-330.

Dvorak, G.J. (1992): Transformation Field Analysis of Inelastic Composite Materials. *Proceedings: Mathematical and Physical Sciences*, Vol. 437, No. 1900, pp.311-327.

Dugdale, DS. (1960): Yielding of steel sheets containing slits. *Nonlinear Dynamics* Vol. , pp. 100–104.

Eshelby, J.D. (1957): The determination of the elastic field of an ellipsoidal inclusion and related problems. *Proceedings of the Royal Society of London.* Series A, Mathematical and Physical Sciences, Vol. 241, No. 1226, pp. 376-396.

Foulk, J.W.; Allen, D.H.; Helms KLE (2000): Formulation of a three dimensional cohesive zone model for application to a finite elements algorithm. *Comp Meth in Appl Mech and Engng*, Vol. 183, pp. 51–67.

Gamstedt, E.K.; Sjorgen, B.A. (1999): Micromechanisms in tension-compression fatigue of composite laminates containing transverse plies. *Composites Science and Technology*, Vol. 59, pp. 167-178.

Gonzalez, C.; Llorca, J. (2006): Multiscale modeling of fracture in fiber-reinforced composites. *Acta Materialia*, Vol. 54, pp. 4171–4181.

Hashin, Z. (1983): Analysis of composite materials – A survey. *J Appl Mech*, Vol. 50, pp. 481–505.

Hillerborg, A.; Modeer, M.; Petersson, P.E. (1976): Analysis of crack formation and crack growth in concrete by means of fracture mechanics and finite elements. *Cement and Concrete Research,* Vol. 6, pp. 773–82.

Kurnatowski, B.; Matzenmiller, A. (2012): Coupled two scale analysis of fiber reinforced composite structures with microscopic damage evolution. *International Journal of Solids and Structures* Vol. 49, pp. 2404–2417.

Ladeveze, P.; Guitard, L.; Champaney, L.; Aubard, X. (2000): Debond modeling for multidirectional composites. *Comp Meth in App Mech and Engng. 1,* Vol. 83, pp. 109–22.

McCartney, A.N.; Kelly, A. (2007): Effective thermal and elastic properties of [+?/- ?] laminates. *Composites Science and Technology,* Vol. 67, pp. 646–661.

Michel, J.C.; Suquet, P. (2003): Non-uniform transformation field analysis. International Journal of Solids and Structures, Vol. 40, pp. 6937–6955.

Mishnaevsky, L.; Brondsted, P. (2007): Micromechanical modeling of strength and damage of fiber reinforced composites. Annual Report on EU FP6 Project UpWind Integrated Wind Turbine Design (WP 3.2).

Naghipour, P.; Bartsch, M.; Voggenreiter, H. (2011): Simulation and experimental validation of mixed mode delamination in multidirectional CF/PEEK laminates under fatigue loading. *International Journal of Solids and Structures*, Vol. 48, pp. 1070–1081.

Paley, M.; Aboudi, J. (1992): Micormechanical analysis of composites by the generalized cells model. *Mech of Materials*. Vol. 14, pp. 127-139.

Paris, P.; Erdogan, F. (1963): Critical analysis of propagation laws. J. Basic Eng, Vol. 85, pp. 528–534.

Pineda, E.J.; Bednarcyk, B.A.; Waas. A. M.; Arnold, S. M. (2013): Mesh Objective Progressive Failure of a Unidirectional Fiber-reinforced Composite Using the Method of Cells. *Int. J. Solids and Structures* (in publishing).

Pineda, E.J.; Bednarcyk, B.A.; Waas, A. M.; Arnold, S. M. (2012): Progressive failure of a unidirectional fiber-reinforced composite using the method of cells: Discretization objective computational results. *NASA/TM*—2012-217649.

Pineda, E.J.(2012): A Novel Multiscale Physics-Based Progressive Damage and Failure Modeling Tool for Advanced Composite Structures. Ph.D. Thesis, University of Michigan, Ann Arbor.

Sankurathri, A.; Baxter, S.; Pindera, M-J. (1996): The effect of fiber architecture on the inelastic response of metal matrix composites with interfacial and fiber damage, in Damage and Interfacial Debonding in Composites edited by G. Z. Voyiadjis and D. H. Allen.

Sun, C.T.; Vaidya, R.S. (1996): Prediction of composite properties from a representative volume element. *Composites Science and Technology,* Vol. 5, pp. 171-179.

Totry, E.; Molina-Aldareguía, J.M.; González, C.; LLorca, J.. (2010): Effect of fiber, matrix and interface properties on the in-plane shear deformation of carbon-fiber reinforced composites. *Composites Science and Technology* Vol. 70, pp. 970–980.

Totry, E.; González, C.; LLorca, J. (2008): Influence of the loading path on the strength of fiber-reinforced composites subjected to transverse compression and shear. *International Journal of Solids and Structures* Vol. 45, pp. 1663–1675.

Totry, E.; González, C.; LLorca, J. (2008): Failure locus of fiber-reinforced composites under transverse compression and out-of-plane shear. *Composites Science and Technology* Vol. 68, pp. 829–839.

Turon, A.; Camanho, P.P.; Costa, J.; Davila, C.G. (2006): A damage model for the simulation of delamination under variable-mode loading. *Mech of Materials.* Vol. 38, pp. 1072–1089.